

# Limit analysis of a shallow subway tunnel with staged construction

Shengbing Yu<sup>\*1,2,3</sup>

<sup>1</sup>School of Civil Engineering and Water Conservancy, Ningxia University, Yinchuan 750021, China

<sup>2</sup>Engineering Research Center of Efficient Use of Water Resources in Arid Modern Agriculture, Ministry of Education, Yinchuan 750021, China

<sup>3</sup>Ningxia Irrigation and Water Resources Control Engineering Technology Research Center, Yinchuan 750021, China

(Received September 29, 2017, Revised January 12, 2018, Accepted January 27, 2018)

**Abstract.** This paper presents a limit analysis of the series of construction stages of shallow tunneling method by investigating their respective safety factors and failure mechanisms. A case study for one particular cross-section of Beijing Subway Line 7 is undertaken, with a focus on the effects of multiple soil layers and construction sequencing of dual tunnels. Results show that using the step-excavation technique can render a higher safety factor for the excavation of a tunnel compared to the entire cross-section being excavated all at once. The failure mechanisms for each different construction stage are discussed and corresponding key locations are suggested to monitor the safety during tunneling. Simultaneous excavation of dual tunnels in the same cross-section should be expressly avoided considering their potential negative interactions. The normal and shear forces as well as bending moment of the primary lining and locking anchor pipe are found to reach their maximum value at Stage 6, before closure of the primary lining. Designing these struts should consider the effects of different construction stages of shallow tunneling method.

**Keywords:** limit analysis; strength reduction; shallow tunneling method; stability

## 1. Introduction

Limit analysis on tunneling projects has been of great interests to engineers and academics for several decades. For two dimensional analysis, face and cross-section stability of tunnels are usually studied independently. Face stability of shallow tunnels of various shapes (i.e., circular, square) in geomaterials (i.e., sand, clay) is widely studied using limit analysis, for example by Dormieux and Leca (1990), Sloan (1992), Augarde *et al.* (2003), Wu and Lee (2003), Li, *et al.* (2009), Huang and Song (2013), Han *et al.* (2016b), as well as the cross-section stability (Davis *et al.*, 1980, Mhlhaus, 1985, Sloan and Assadi 1991, Assadi and Sloan 1992, Osman *et al.* 2006, Yamamoto, *et al.*, 2013, Yamamoto *et al.* 2014, Wilson *et al.* 2015). The finite element limit analysis method in particular has been evolved with more efficient nonlinear optimization algorithms and applied for solving single or dual circular and square tunnel problems (Sloan and Assadi 1991, Assadi and Sloan 1992, Yamamoto *et al.* 2013, Yamamoto *et al.* 2014, Wilson *et al.* 2015, Yang *et al.* 2015). For three dimensional analysis, the face stability of circular or non-circular tunnels have been studied and revisited by using 3D collapse mechanisms (Rendus *et al.* 2002, Soubra *et al.* 2008, Mollon *et al.* 2011, Ibrahim *et al.* 2015, Zhang *et al.* 2015, Han *et al.* 2016a, Pan and Dias 2017).

Recently the shallow tunneling method (STM) (Xiang *et*

*al.* 2005, Fang *et al.* 2011, Fang *et al.* 2012, Fang *et al.* 2015, Hou *et al.* 2015, Liu *et al.* 2015) has gained a lot of interests from engineers. The shallow tunneling method relies on manpower excavation and is particularly suitable for the construction of shallow tunnels in densely built urban area, for which the road alignment, topographic and geologic conditions makes the conventional shield tunneling method more difficult. The main advantage of the shallow tunneling method over conventional shield tunneling techniques is its outstanding flexibility, allowing the use of many different support techniques (e.g., pretunneling techniques (Peila *et al.* 1995) or forepoling with grouting) and minimum width requirement in order to perform construction. The shallow tunneling method was first acknowledged by China's Ministry of Construction in 1987 and since then it has been widely employed in tunneling projects in urban areas. Accumulated engineering experience demands corresponding theoretical and numerical investigation of the shallow tunneling approach. However, to date there have been few such studies using limit analysis on this new tunneling method, specifically no numerical investigation with considering staged excavation and locking anchor pipes. This paper aims to describe the limit analysis of a horseshoe shaped tunnel constructed by using the shallow tunneling method. Step-excavation techniques are examined, considering the stability and failure mechanisms of different excavation stages. A case study of a cross-section in the Beijing Subway Line 7 is provided to illustrate the failure mechanism of each stage. This study is expected to provide guidelines for practical engineering.

---

\*Corresponding author, Associate Professor  
E-mail: shengbingyu@nxu.edu.cn or  
shengbingyu@outlook.com

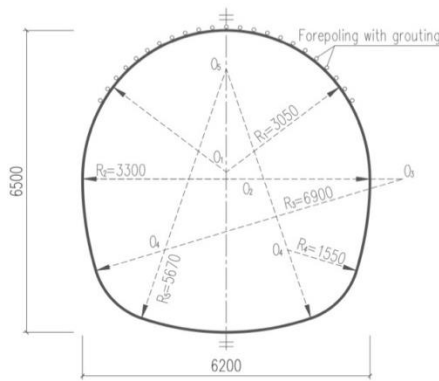


Fig. 1 Geometry of cross-section of the tunnel (Unit: mm)

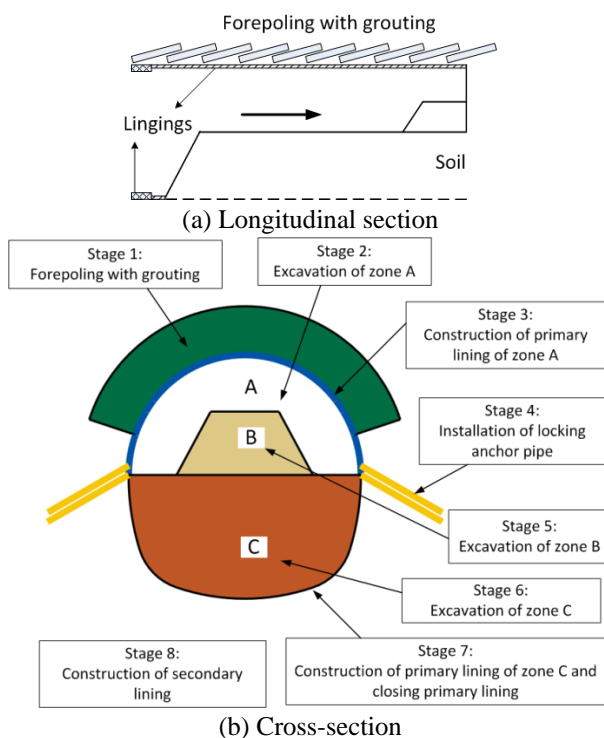


Fig. 2 Construction stages of the tunnel

## 2. Problem description

For the shallow tunneling method, the shape of the tunnel cross-section and its construction procedure varies significantly, depending on tunnel function requirements and local topographic and geologic conditions (Fang *et al.* 2012). In this paper the stability of a horseshoe shaped tunnel constructed using the step-excavation technique is investigated. Fig. 1 shows the geometry details of the tunnel cross-section, which consists of eight arc pieces. In contrast to the shield tunneling technique, manpower-excavation is used in the shallow tunneling method and a total of eight stages are required to complete the construction of the entire cross-section (see Fig. 2(b)). Forepoling with grouting is first used to reinforce the soil in the area above the tunnel before further excavation, as shown in Fig. 1 and Fig. 2(a). The length of forepoling pipes is 2.5 m. Tunnel excavation is then carried out in steps (see Fig. 2). The soil in Area A is excavated first, with subsequent installation of

primary lining of the upper part of the tunnel. Following this the soil in Area B and Area C is excavated and supported in sequence. With the advance of tunnel excavation, new forepoling pipes are driven into the soil with a minimum overlap length of 1 m.

## 3. Finite element limit analysis and strength reduction

Limit analysis is an efficient tool for rapid assessment of the stability of geotechnical structures without performing a step-by-step elastoplastic analysis. Based on the static and kinematic theorems of classical plasticity theory developed by Gvozdev (1960) and Drucker *et al.* (1952), limit analysis assumes small deformations, a perfectly plastic material and an associated flow rule. A lower bound approach estimates the actual collapse load from below while an upper bound approach provides its estimate from above for a perfectly plastic material. By using accurate lower and upper bound estimates, the actual collapse load can be bracketed in a very narrow range. Rigorous lower and upper bounds can be obtained by using the finite element limit analysis method (Sloan 1988, 1989, Sloan and Kleeman 1995, Lyamin and Sloan 2002a, Lyamin and Sloan 2002b, Krabbenhoft *et al.* 2005, Sloan 2013) and these formulations have been successfully used so far to perform stability analysis for various tunnels (Yamamoto *et al.* 2011, 2013, 2014, Wilson *et al.* 2015). The strength reduction analysis aims to compute a strength reduction factor by which the original material strength parameters (for soil this usually means cohesion and friction angle) are reduced in order to attain a state of collapse. For Mohr-Coulomb type materials which are used for all soil layers in the considered cases, soil cohesion  $c$  and friction angle  $\tan\phi$  are reduced by the same amount, as in Eq. 1. Strength reduction problems combined with finite element limit analysis is reported by Sloan (2013) and revisited by Krabbenhoft and Lyamin (2015). Readers are referred to these original published papers for further details.

$$\text{Safety factor} = \frac{c}{c_{\text{reduced}}} = \frac{\tan\phi}{\tan\phi_{\text{reduced}}} \quad (1)$$

## 4. Numerical modeling

For simplicity, step-excavation of the tunnel is considered as a plane strain problem, with a focus on the comparison of tunnel stability at different excavation stages. Neglecting the potential three dimensional effect would unavoidably render an underestimation of the safety factors of practical tunnel excavation. However, from a practical point of view, the results obtained in this study will be conservative. According to the construction scheme and boundary conditions, five stages of tunnel excavation are considered herein (see Fig. 3). Stages 2, 5 and 6 are studied here according to the construction scheme shown in Fig. 2. For comparison, two hypothetical stages, 2(5) and stage 2(6), are examined to show the effects of step-excavation techniques. Stage 2(5) combines the excavation work of

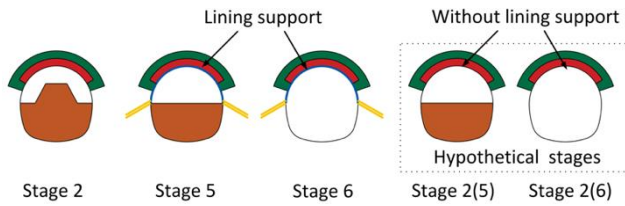


Fig. 3 Numerical simulation stages

Table 1 Physical and mechanical properties of soils and struts

	Thickness (m)	Specific weight (kN/m <sup>3</sup> )	Cohesion (kPa)	Internal friction angle (°)
Equivalent layer 1	0.65	21	200	30
Equivalent layer 2	0.65	20	46	38
Primary lining	0.25	25		

stage 2 and stage 5 together. Stage 2(6) assumes that the excavation of the entire cross-section is conducted all at once without using step-excavation techniques. Primary lining support in the upper part of the tunnel cross-section, as shown in Fig. 3, is considered for stage 5 and stage 6, but neglected for stages 2(5) and 2(6).

As commonly known, forepoling with grouting technology is used to reinforce the soil above the tunnel before excavation and these forepoling pipes are installed in a longitudinal direction in relation to the tunnel. In this study two equivalent layers of uniform Mohr–Coulomb materials are considered to model the effect of forepoling with grouting. For equivalent layer No. 1, the emphasis is placed on the effect of densely installed steel pipes and the reinforcement effect of grouting. For equivalent layer No. 2, the effects of grout propagation and soil reinforcement are of interests. The mechanical properties of equivalent layers are estimated by using the average value of field test data for the grouting in soils. The total cross-section area of steel pipes are also a factor considered when estimate the cohesion value for the equivalent layer No. 1. For the purposes of this study the grouting material used is soluble silicate. The primary lining and locking anchor pipes are simulated by plate elements and nail rows respectively. The out-of-plane spacing of locking anchor pipes (DN32, L = 2.5 m) is 0.5 m and yield force is 200 kN/m. Details and values of all parameters can be found in Table. 1. As our main concern in this case is the collapse risk introduced by weak layers of natural soil profiles, no strength reduction is applied to equivalent layer No. 1, equivalent layer No. 2 and the strut parts (e.g., concrete lining and locking anchor pipes). In the following numerical studies, the soil profiles and depths of the tunnels will vary, with the size of tunnel cross-section and related construction stages all remaining the same.

## 5. Numerical analysis and results

A homogenous soil profile is first considered to examine the safety factors and failure mechanisms of a single tunnel. Then a case study of a cross-section of Beijing Subway Line 7 is performed, examining the effects of multiple soil

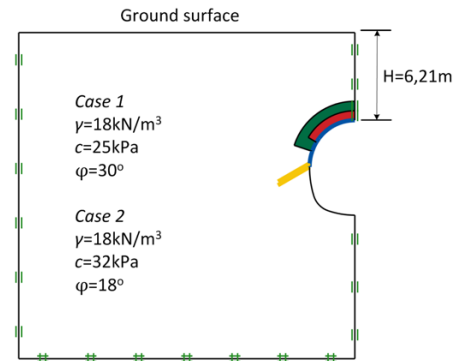
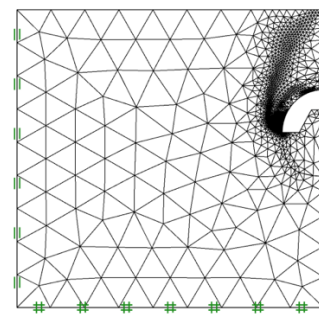


Fig. 4 Numerical modelling of the tunnel in homogenous soil profile

Fig. 5 Typical mesh in homogenous soil ( $H = 6$  m, stage 2)

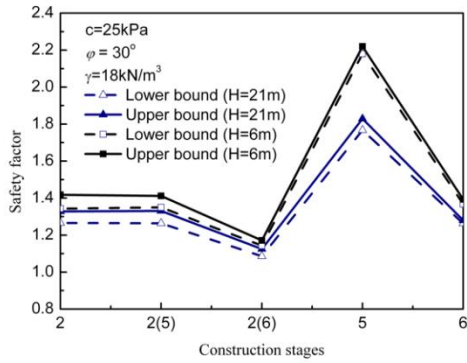
layers and dual tunnels geometry.

### 5.1 Homogenous soil profile

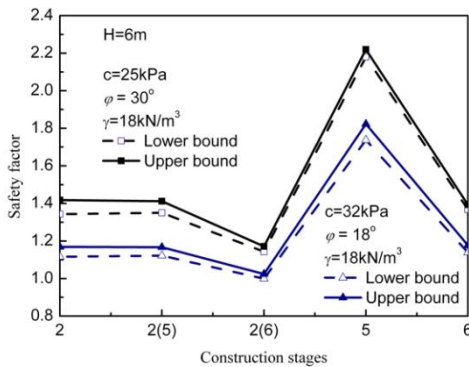
As depicted in Fig. 4, the ground is modelled as a uniform Mohr–Coulomb material, with two different sets of material parameters and considering two extreme cases of tunnel buried depth  $H$ . Note that the tunnel buried depth  $H$  is defined as the vertical distance from the ground surface to the top of the tunnel. The boundary conditions are also shown in Fig. 4. Only half of the geometry is modelled considering the symmetry of tunneling. Finite element mesh is adaptively used by default in all performed computations and a typical adapted mesh is shown in Fig. 5.

The lower and upper bound solutions of stability factors for all construction stages are shown in Fig. 6. It can be seen that the values of upper and lower bound solutions are very close to each other. Therefore, it is deemed acceptable to discuss stability factors without specifying upper or lower bound approach. Fig. 6 illustrates that the stability factor of Stage 5 is the highest, but that of Stage 2(6) is the lowest among all stages. Comparatively, the stability factors of Stage 2 and Stage 2(5) are basically the same, indicating that retaining soil of Area B (as shown in Fig. 2) has essentially no effect on tunnel cross-section stability. Note that retaining soil of Area B may contribute to maintain the tunnel face stability and it is out of interest of this paper. Regarding the effects of tunnel buried depth  $H$  and soil strength properties, no apparent changes in stability factors are observed in Fig. 6, all results implying that Stage 2(6) is the most dangerous of all simulation stages considered.

The failure mechanisms for each stage of tunneling are

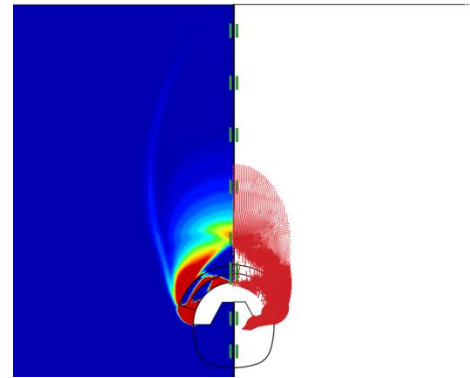


(a) For different buried depth  $H$

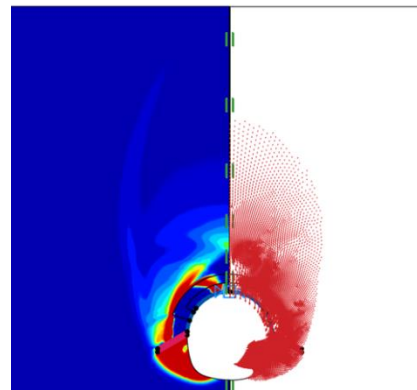


(b) For different soil strength

Fig. 6 Safety factors for different construction stages

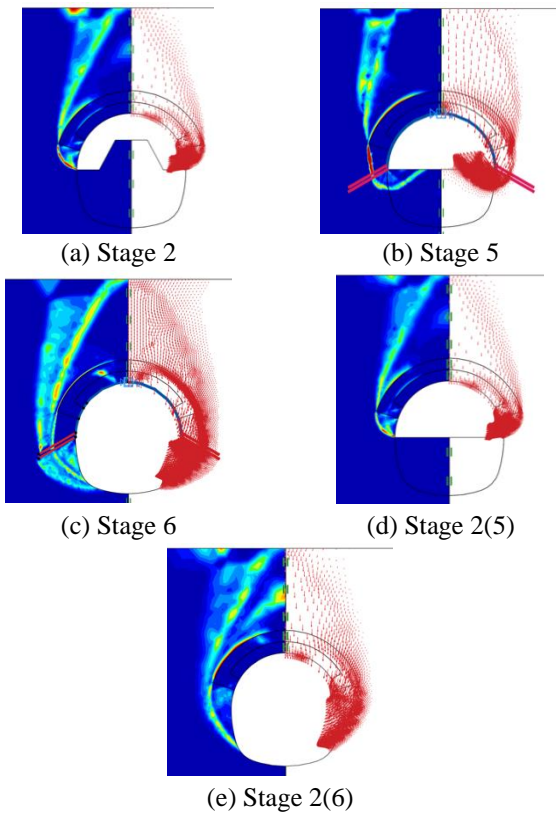


(a) Stage 2



(b) Stage 6

Fig. 8 Local failure mechanism ( $H = 21$  m): total dissipation field (left) and velocity field (right)



(a) Stage 2

(b) Stage 5

(c) Stage 6

(d) Stage 2(5)

(e) Stage 2(6)

Fig. 7 Failure mechanism ( $H = 6$  m): plastic multiplier field (left) and velocity field (right)

analyzed in Fig. 7 using plastic multiplier field and velocity

field of the upper bound solution. Similar failure mechanisms are observed for Stage 2 and Stage 2(5), confirming that retaining the soil of Area B has no significant influence on tunnel cross-section stability. It can be seen from Fig. 7(b), 7(c), 7(d) and 7(e) that the application of lining support and locking anchor pipes tends to induce the potential failure of soil at the sides of the tunnel to move and extend outward. It indicates that the lining support and locking anchor pipes are not only able to prevent the soil from falling from above, but also to increase the stability for subsequent construction stages. Since possible failures might occur in the foot edge (stage 2), ground (stage 5), and side (stage 6) of the excavation face, corresponding in-situ measurements should be conducted during tunnel excavation to ensure safety. Additional internal supports can also be implemented according to these failure mechanisms. For example, grouting can be used to reinforce the soil in the vicinity of these critical locations. Temporary strut supports can be installed to alleviate the pressure from the tunnel crown, especially for Stage 6 where the primary lining of the upper part of the tunnel cross-section has already been implemented.

Fig. 8 shows the total dissipation and velocity fields of stages 2 and 6 under the influence of buried depth  $H$ . As seen, the velocity field does not extend to the ground surface and a local failure mechanism is mobilised, which also explains the insignificance of buried depth  $H$  on the safety factors, as depicted in Fig. 6(a).

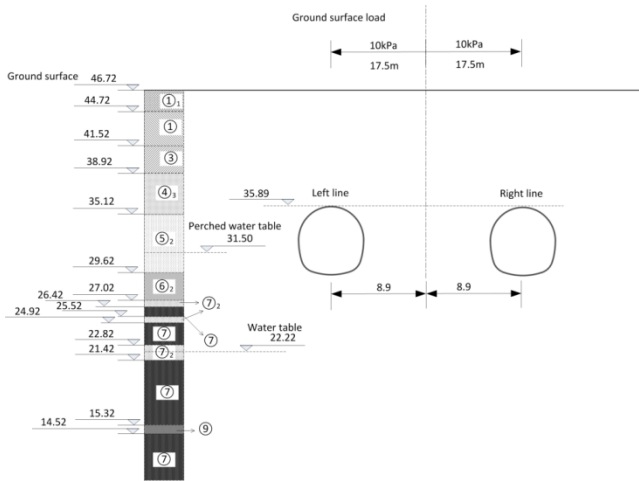


Fig. 9 Tunnel cross-section and geological profile of the site

Table 2 Physical and mechanical properties of soils and reinforced layers with grouting

		Specific weight (kN/m <sup>3</sup> )	Cohesion (kPa)	Internal friction angle (°)
① <sub>1</sub>	Miscellaneous fill	16.0	5.0	10.0
①	Silt fill	16.5	8.0	19.3
③	Silt	19.4	11.3	29.3
④ <sub>3</sub>	Fine sand	20.1	0	32.0
⑤ <sub>2</sub>	Fine sand	20.1	0	32.0
⑥ <sub>2</sub>	Silt	20.0	16.7	27.3
⑦ <sub>2</sub>	Fine sand	20.3	0	36.0
⑦	Gravel	21.5	0	45.0
⑨	Gravel	21.7	0	48.0
	Curtain grouting in sand	20.5	38.0	30.0
	Curtain grouting in silt	20.4	36.0	29.0

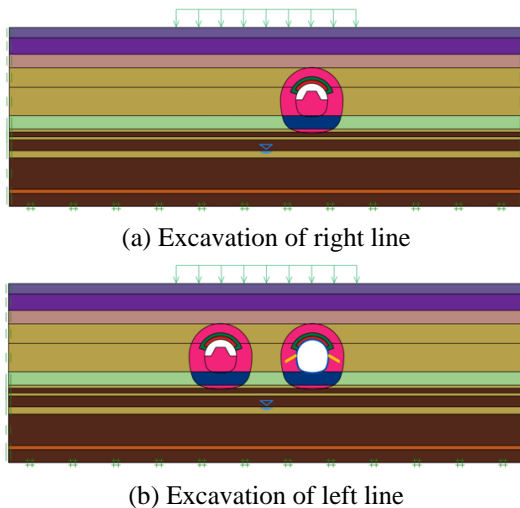


Fig. 10 Numerical modelling of a cross-section of Beijing Subway Line 7

5.2 Case study

Considering the distinctly different geological

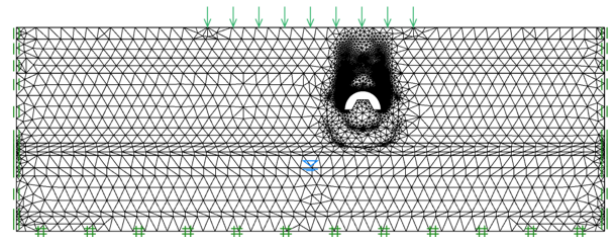


Fig. 11 Typical mesh for a cross-section of Beijing Subway Line 7 (right line, stage 2)

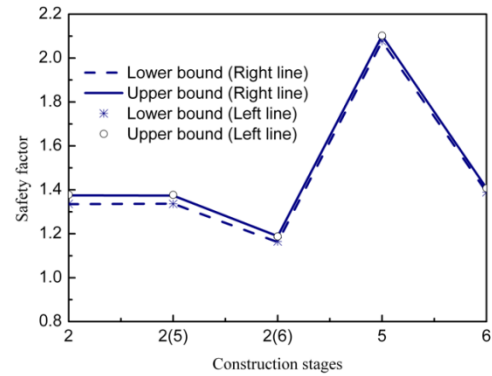


Fig. 12 Safety factors for a tunnel cross-section of Beijing Subway Line 7

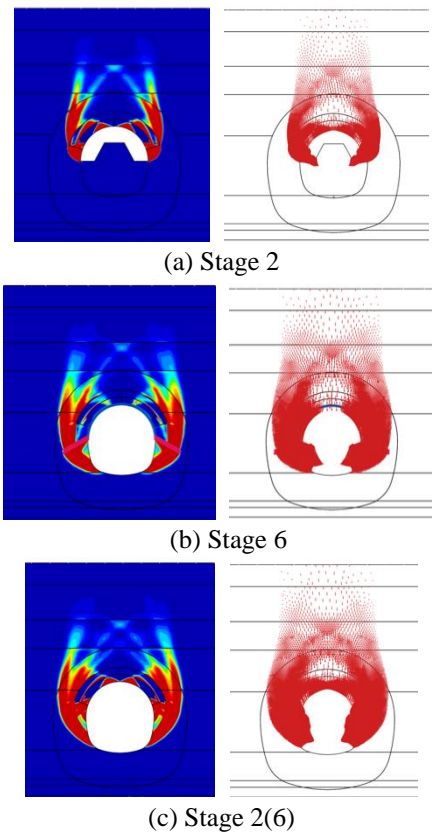


Fig. 13 Failure mechanism of right line (Upper bound): shear dissipation field (left) and velocity field (right)

conditions and surrounding environment, practical excavation of a tunnel is much more complex than suggested in the numerical examples shown above. In the

following case study, a cross-section of Beijing Subway Line 7 is examined.

Fig. 9 illustrates two identical horseshoe shaped tunnels, between which the distance is 17.8 m. The magnitude of loading on the ground surface above the tunnels is set to 10 kN/m. Geological investigation (see Fig. 9) shows that the main excavation of the tunnels is in the fine sand layer, where a perched water table is found. Special treatment must first be conducted to ensure that all manpower excavation will be performed under a no-water-leaking environment. Dewatering and curtain grouting technologies are combined to reinforce the soil in the vicinity of the tunnel. Application of curtain grouting is also able to decrease the permeability of the fine sand layer so that the residual water in this layer will not significantly affect the excavation work. In the model, curtain grouting is modelled as a layer of uniform Mohr-Coulomb material around the tunnel, the thickness of which is 3 m. Details of the physical and mechanical properties of soils and grouting layers can be found in Table 2.

In practice, the advanced heads of the left and right tunnel lines are kept at least a distance of 35 m apart in the longitudinal direction. The right tunnel line is the first to be excavated for Beijing Subway Line 7. Once the primary lining of the right line has been installed, the excavation of the left tunnel line can begin. Corresponding numerical models and boundary conditions for this sequential tunneling procedure are shown in Fig. 10. Additionally, another hypothetical case, in which both left and right tunnel lines are excavated simultaneously at one cross-section, is simulated to highlight the most negative effect of interactions for the dual tunnels. A typical mesh is depicted in Fig. 11.

Lower and upper bound solutions of safety factors for both right and left lines are provided in Fig. 12. It can be seen that the safety factors of the two lines for each construction stage are basically the same, indicating that maintaining a proper distance of the advanced heads for dual tunnel excavation can avoid the possible negative influence of ongoing dual tunnel excavation in the same cross-section. The variation of safety factors between different construction stages seems to correspond with the findings previously obtained for the homogenous soil profile case. The hypothetical stage 2(6) still gives the lowest safety factor, thus requiring more emphasis on Stage 2 and Stage 6 in practice. The failure mechanisms for the right tunnel line are shown in Fig. 13. It can be seen that the failure mechanisms for multiple layers of soil do not change significantly when compared to those for the homogenous soil profile analysed previously. Taking into account the relatively large distance between the two tunnel lines in this case, similar failure mechanisms are automatically achieved. It can be seen that the failure mostly occurs in the reinforced soil layers and the influence of the existing right line on the left line is largely restrained.

Failure mechanisms of two tunnels which are excavated simultaneously in the same cross-section are illustrated in Fig. 14. An apparent difference in failure mechanisms is observed, indicating strong negative interaction between the simultaneous excavations of two tunnels, which should be avoided in practical engineering.

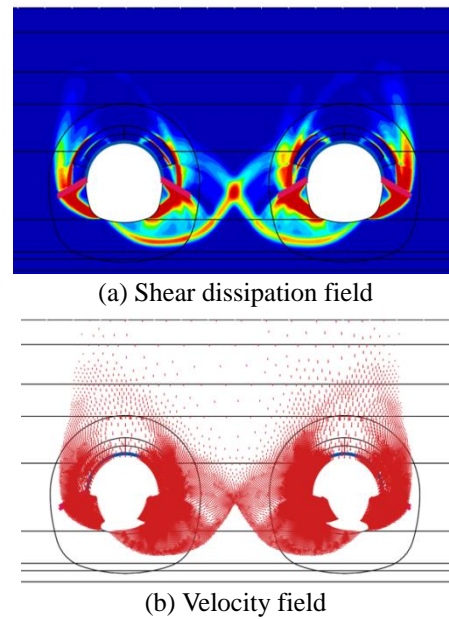


Fig. 14 Failure mechanism of two tunnels excavated at the same time (Stage 6)

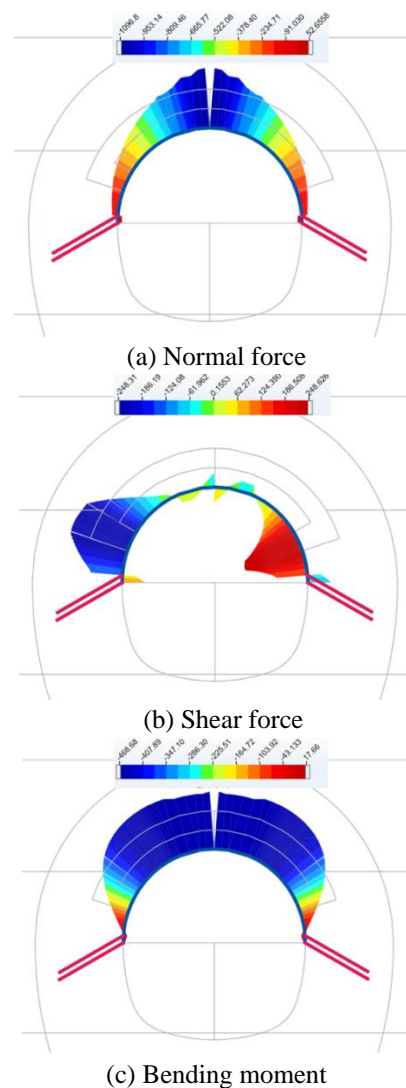


Fig. 15 Normal, shear force and bending moment of primary lining for right line (Stage 5, Unit: kN or kN/m)

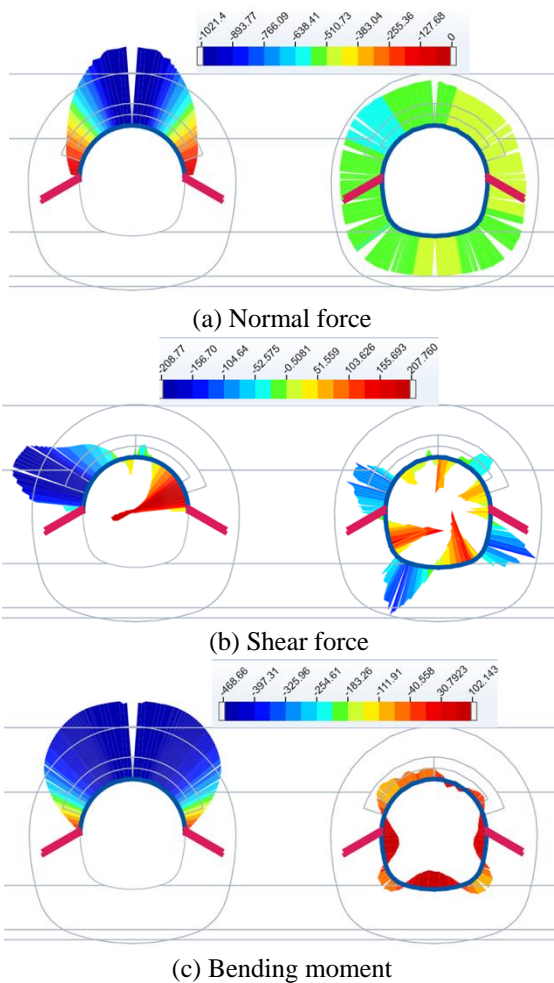


Fig. 16 Normal, shear force and bending moment of primary lining for left line (Stage 6, Unit: kN or kN/m)

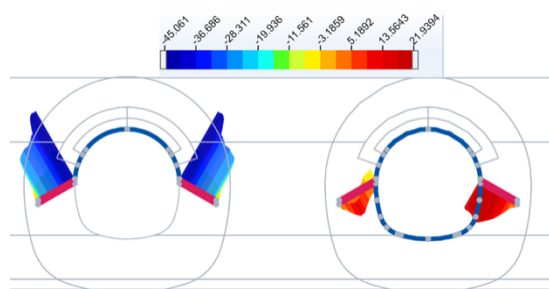


Fig. 17 Normal force of locking anchor pipe for left line (Stage 6, Unit: kN)

Primary lining for the shallow tunneling method, unlike the shield tunneling method, is constructed in steps. Normal and shear forces and the bending moment of the primary lining are shown in Fig. 15 and 16 for Stages 5 and 6 respectively. It can be seen in Fig. 16 that the maximum values of normal and shear forces and bending moment of the primary lining for the left line are much larger than those for the already constructed right line. It indicates that the forces in the primary lining can be very different before closure of the primary lining. Proper safety checks of the primary lining design should be conducted with respect to the un-closed state, namely in Stage 5 and Stage 6. The

normal force of the locking anchor pipe for the already constructed right line also appears smaller than that for the left line, as shown in Fig. 17. This indicates that safety check of the locking anchor pipe design should be conducted with respect to Stage 6.

## 5. Conclusions

This paper presents a limit analysis of a shallow subway tunnel, the construction of which employs manpower for excavation. Step-excavation techniques are analyzed in terms of the safety factors of different construction stages. Upper and lower bound solutions of safety factors are compared and different failure mechanisms are examined. A case study of a cross-section of Beijing Subway Line 7 is investigated in this paper considering effects of multiple layers of soil and the construction sequencing of dual tunnels. It shows that by using step-excavation techniques the excavation of the tunnel can be safer than the hypothetical case of excavating the entire cross-section all at once. The failure mechanisms of each stage are discussed in this paper and critical locations in the tunnel cross-section are provided for in-situ construction safety monitoring. When dual tunnels are considered, the excavation of both lines at the same time in the same cross-section should be expressly avoided due to the potential negative interactions. The normal and shear forces, as well as the bending moment of the primary lining and locking anchor pipe reach their maximum values at Stage 6. Therefore, the design of these struts for steps-excavated tunnels should be performed considering all progression stages.

## Acknowledgments

The author acknowledges the financial support provided by the Ningxia excellent college discipline construction project: water conservancy (No. NXYLXK2017A03), and project 2018AAC03005.

## References

- Assadi, A. and Sloan, S.W. (1992), "Undrained stability of shallow square tunnel", *J. Geotech. Eng.*, **117**(8), 1152-1173.
- Augarde, C.E., Lyamin, A.V. and Sloan, S.W. (2003), "Stability of an undrained plane strain heading revisited", *Comput. Geotech.*, **30**(5), 419-430.
- Davis, E.H., Mair, R.J., Seneviratne, H.N. and Gunn, M.J. (1980), "The stability of shallow tunnels and underground openings in cohesive material", *Geotechnique*, **30**(4), 397-416.
- Dormieux, L. and Leca, E. (1990), "Upper and lower bound solutions for the face stability of shallow circular tunnels in frictional material", *Geotechnique*, **40**(4), 581-606.
- Drucker, D.C., Prager, W. and Greenberg, H.J. (1952), "Extend limit design theorems for continuous media", *Quart. Appl. Math.*, **9**(4), 381-389.
- Fang, Q., Zhang, D., Li, Q. and Wong, L.N.Y. (2015), "Effects of twin tunnels construction beneath existing shield-driven twin tunnels", *Tunn. Undergr. Sp. Technol.*, **45**, 128-137.

- Fang, Q., Zhang, D. and Wong, L.N.Y. (2011), "Environmental risk management for a cross interchange subway station construction in China", *Tunn. Undergr. Sp. Technol.*, **26**(6), 750-763.
- Fang, Q., Zhang, D., and Wong, L.N.Y. (2012), "Shallow tunnelling method (stm) for subway station construction in soft ground", *Tunn. Undergr. Sp. Technol.*, **29**, 10-30.
- Gvozdev, A.A. (1960), "The determination of the value of the collapse load for statically indeterminate systems undergoing plastic deformation", *J. Mech. Sci.*, **1**(4), 322-335.
- Han, K., Zhang, C., Li, W. and Guo, C. (2016a), "Face stability analysis of shield tunnels in homogeneous soil overlaid by multilayered cohesive-frictional soils", *Math. Prob. Eng.*
- Han, K., Zhang, C. and Zhang, D. (2016b), "Upper-bound solutions for the face stability of a shield tunnel in multilayered cohesive-frictional soils", *Comput. Geotech.*, **79**, 1-9.
- Hou, Y., Fang, Q., Zhang, D., and Wong, L.N.Y. (2015), "Excavation failure due to pipeline damage during shallow tunnelling in soft ground", *Tunn. Undergr. Sp. Technol.*, **46**, 76-84.
- Huang, M. and Song, C. (2013), "Upper-bound stability analysis of a plane strain heading in non-homogeneous clay", *Tunn. Undergr. Sp. Technol.*, **38**, 213-223.
- Ibrahim, E., Soubra, A.H., Mollon, G., Raphael, W., Dias, D. and Reda, A. (2015), "Three-dimensional face stability analysis of pressurized tunnels driven in a multilayered purely frictional medium", *Tunn. Undergr. Sp. Technol.*, **49**, 18-34.
- Krabbenhoft, K. and Lyamin, A.V. (2015), "Strength reduction finite-element limit analysis", *Geotech. Lett.*, **5**(4), 250-253.
- Krabbenhoft, K., Lyamin, A.V., Hjiij, M. and Sloan, S.W. (2005), "A new discontinuous upper bound limit analysis formulation", *J. Numer. Meth. Eng.*, **63**(7), 1069-1088.
- Li, Y., Emeriault, F., Kastner, R. and Zhang, Z.X. (2009), "Stability analysis of large slurry shield-driven tunnel in soft clay", *Tunn. Undergr. Sp. Technol.*, **24**(4), 472-481.
- Liu, J., Wang, F., He, S., Wang, E. and Zhou, H. (2015), "Enlarging a large-diameter shield tunnel using the pile-beam-arch method to create a metro station", *Tunn. Undergr. Sp. Technol.*, **49**, 130-143.
- Lyamin, A.V. and Sloan, S.W. (2002a), "Lower bound limit analysis using non-linear programming", *J. Numer. Meth. Eng.*, **55**(5), 573-611.
- Lyamin, A.V. and Sloan, S.W. (2002b), "Upper bound limit analysis using linear finite elements and non-linear programming", *J. Numer. Anal. Meth. Geomech.*, **26**(2), 181-216.
- Mhlhaus, H.B. (1985), "Lower bound solutions for circular tunnels in two and three dimensions", *Rock Mech. Rock Eng.*, **18**(1), 37-52.
- Mollon, G., Dias, D. and Soubra, A.H. (2011), "Rotational failure mechanisms for the face stability analysis of tunnels driven by a pressurized shield", *J. Numer. Anal. Meth. Geomech.*, **35**(12), 1363-1388.
- Osman, A.S., Mair, R.J. and Bolton, M.D. (2006), "On the kinematics of 2d tunnel collapse in undrained clay", *Géotechnique*, **56**(9), 585-595.
- Pan, Q. and Dias, D. (2017), "Upper-bound analysis on the face stability of a non-circular tunnel", *Tunn. Undergr. Sp. Technol.*, **62**, 96-102.
- Peila, D., Oreste, P.P., Rabajoli, G. and Trabucco, E. (1995), "The pretunnel method, a new Italian technology for full-face tunnel excavation: A numerical approach to design", *Tunn. Undergr. Sp. Technol.*, **10**(3), 367-374.
- Subrin, D. and Wong, H. (2002), "Tunnel face stability in frictional material: A new 3d failure mechanism", *Comptes Rendus Mécanique*, **330**(7), 513-519.
- Sloan, S.W. (1988), "Lower bound limit analysis using finite-elements and linear-programming", *J. Numer. Anal. Meth. Geomech.*, **12**(1), 61-77.
- Sloan, S.W. (1989), "Upper bound limit analysis using finite-elements and linear-programming", *J. Numer. Anal. Meth. Geomech.*, **13**(3), 263-282.
- Sloan, S.W. and Assadi, A. (1992), "Undrained stability of a plane strain heading", *Can. Geotech. J.*, **31**(3), 443-450.
- Sloan, S.W. (2013), "Geotechnical stability analysis", *Geotechnique*, **63**(7), 531-571.
- Sloan, S.W. and Assadi, A. (1991), "Undrained stability of a square tunnel in a soil whose strength increases linearly with depth", *Comput. Geotech.*, **12**(4), 321-346.
- Sloan, S.W. and Kleeman, P.W. (1995), "Upper bound limit analysis using discontinuous velocity-fields", *Comput. Meth. Appl. Mech. Eng.*, **127**(1-4), 293-314.
- Soubra, A.H., Dias, D., Emeriault, F. and Kastner, R. (2008), "Three-dimensional face stability analysis of circular tunnels by a kinematical approach", *Proceedings of the GeoCongress 2008*, New Orleans, Louisiana, U.S.A., March.
- Wilson, D.W., Abbo, A.J., Sloan, S.W. and Lyamin, A.V. (2015), "Undrained stability of dual square tunnels", *Acta Geotech.*, **10**(5), 665-682.
- Wu, B.R. and Lee, C.J. (2003), "Ground movements and collapse mechanisms induced by tunneling in clayey soil", *J. Phys. Modell. Geotech.*, **3**(4), 15-29.
- Xiang, Y., He, S., Cui, Z. and Ma, S. (2005), "A subsurface drift and pile protection scheme for the construction of a shallow metro tunnel", *Tunn. Undergr. Sp. Technol.*, **20**(1), 1-5.
- Yamamoto, K., Lyamin, A.V., Wilson, D.W., Sloan, S.W. and Abbo, A.J. (2011), "Stability of a single tunnel in cohesive-frictional soil subjected to surcharge loading", *Can. Geotech. J.*, **48**(12), 1841-1854.
- Yamamoto, K., Lyamin, A.V., Wilson, D.W., Sloan, S.W. and Abbo, A.J. (2013), "Stability of dual circular tunnels in cohesive-frictional soil subjected to surcharge loading", *Comput. Geotech.*, **50**, 41-54.
- Yamamoto, K., Lyamin, A.V., Wilson, D.W., Sloan, S.W. and Abbo, A.J. (2014), "Stability of dual square tunnels in cohesive-frictional soil subjected to surcharge loading", *Can. Geotech. J.*, **51**(8), 829-843.
- Yang, F., Zhang, J., Yang, J., Zhao, L. and Zheng, X. (2015), "Stability analysis of unlined elliptical tunnel using finite element upper-bound method with rigid translatory moving elements", *Tunn. Undergr. Sp. Technol.*, **50**, 13-22.
- Zhang, C., Han, K. and Zhang, D. (2015), "Face stability analysis of shallow circular tunnels in cohesive-frictional soils", *Tunn. Undergr. Sp. Technol.*, **50**, 345-357.

CC